

Malic Acid Production by *Aspergillus oryzae*: The effect of Alkaline-Earth Carbonate Buffer Identity

Hendrik Brink*, Monique Geyer-Johnson, Willie Nicol

Department of Chemical Engineering, University of Pretoria, Lynnwood, South Africa
 deon.brink@up.ac.za

Malic acid is a specialty chemical that is currently mainly used in the food and beverage industry (market value of \$182 million) but has a potential market value of \$3.5 billion if used to produce maleic anhydride. The results from the study indicated that the production of malic acid by *A. oryzae* requires the presence of the alkaline earth metals calcium or magnesium in significant quantities. It was observed that replacing an amount of CaCO_3 ($240 \text{ g.l}^{-1} \text{ CaCO}_3$), significantly over that required for pH buffering ($21 \text{ g.l}^{-1} \text{ CaCO}_3$), with an equivalent amount of MgCO_3 ($192 \text{ g.l}^{-1} \text{ MgCO}_3$ based on CO_3^{2+}) results in similar malic acid yields and final malic acid titers. In contrast, a marked reduction in glucose consumption and malic acid production rates were observed. These observations are likely due to an evolutionary response to calcareous soils. These soils tend to immobilize minerals in solid precipitates resulting in nutrient depletion, while the production of malic acid solubilizes these minerals making them bioavailable. The higher rates observed for the calcium vs magnesium runs were likely a result of the stimulatory effect of Ca^{2+} on the ATP generating pathways as well as several regulatory responses within the fungal physiology. In addition, it was found that *A. oryzae* was capable of assimilating malic acid from the environment, therefore, minimizing the loss of valuable carbon due to malic acid excretion. This study provides invaluable information required for economically viable malic acid production by *A. oryzae* which could markedly reduce reliance on the petrochemical industry.

1. Introduction

Developing a sustainable society requires a significant industrial shift away from petroleum-based products and towards renewable and bio-based technologies. This shift has been supported by renewed interest by consumers in natural, biodegradable, and environmentally friendly products (Mondala, 2015). As part of its drive towards bio-based products, the US Department of Energy has identified 12 priority platform chemicals required for bio-based chemical production; malic acid – along with the other two four carbon diprotic organic acids succinic- and fumaric acids- being considered among these (Werpy and Petersen, 2004). The current worldwide demand for malate is reported to be 200 kt/a (Chi et al., 2016) while the current international supply of L-malic acid is estimated at 40 kt/a (Liu et al., 2018). Currently, malic acid is commercially produced by the catalytic hydration of maleic or fumaric acid, both derived from maleic anhydride. Maleic anhydride is, in turn, produced from vapor phase oxidation of hydrocarbons, most prominently butane (Hermann and Patel, 2007). Unfortunately, this synthetic pathway produces a racemic mixture of L- and D-malic acid which is unsuitable for the food and beverage industry where malic acid is utilized as an acidulant (Knuf et al., 2014).

The biological production of malic acid provides stereo selectivity since L-malic acid is a key intermediate in the tricarboxylic acid cycle (TCA) present in most microorganisms (Liu et al., 2017). Filamentous fungi of the genus *Aspergilli* are superior producers of various bio-based chemicals including lipases, (Melo et al., 2011) xylanase, (Park et al., 2002), and various organic acids; *Aspergillus flavus* and *A. oryzae* widely considered the best biological producers of malic acid (Ochsenreither et al., 2014). However, *A. flavus* is known to produce hazardous amounts of carcinogenic aflatoxin, making the malic acid produced unsuitable for the food industry. In contrast, *A. oryzae* is a GRAS (Generally Regarded as Safe) organism that does not produce mycotoxins and has therefore been used in the production of sake, shochu, soy sauce, and miso for centuries (Payne et al., 2006).

Currently, laboratory-scale methods for malic acid production are limited due to the use of pellet morphology and CaCO_3 as the go-to buffering agent which complicates downstream processing. Geyer et al. (2018) observed a maximum malic acid production rate of $0.09 \text{ g.l}^{-1}.\text{h}^{-1}$ for $20 \text{ g.l}^{-1} \text{ CaCO}_3$ was initially dosed as compared to a maximum malic acid production rate of $0.23 \text{ g.l}^{-1}.\text{h}^{-1}$ for $100 \text{ g.l}^{-1} \text{ CaCO}_3$. This compares well with the results obtained by Kövilein et al. (2021) who measured a maximum malic acid production rate of $0.052 \text{ g.l}^{-1}.\text{h}^{-1}$ for $10 \text{ g.l}^{-1} \text{ CaCO}_3$ and $0.121 \text{ g.l}^{-1}.\text{h}^{-1}$ for $90 \text{ g.l}^{-1} \text{ CaCO}_3$. These results indicate a likely synergistic effect of excess CaCO_3 on the excretion of malic acid in addition to its role as a pH buffer. To assess the effect of exchanging Ca^{2+} for Mg^{2+} on *A. oryzae* malic acid fermentation, while maintaining the buffering capacity and bicarbonate source in the medium, two different carbonate buffers were compared by adding the same amount of CO_3^{2-} and changing only the cation (Ca^{2+} vs Mg^{2+}). The resulting buffer concentrations used were 240 g/l CaCO_3 and 192 g/l MgCO_3 (impurities of each taken into consideration).

2. Materials and Methods

2.1 Micro-organisms and fermentation in shake flasks

A. oryzae NRRL 3488 was obtained from the Agricultural Research Service Culture Collection in Illinois, USA. The stock cultures were stored at $-40 \text{ }^\circ\text{C}$ in a 50 % w/w glycerol solution. Potato dextrose agar (PDA) (Merck KgaA, Darmstadt, Germany) plates were inoculated with the stock solution and incubated at $30 \text{ }^\circ\text{C}$ for 7 days. Approximately 60 mg of spores (*circa* 6.7×10^8 spores (Smith et al., 1988)) were harvested from two agar plates with sterilized distilled water. The inoculum was prepared by adding the spore solution to a 10 % w/w glycerol solution which was subsequently stored at $-40 \text{ }^\circ\text{C}$.

Production was done using a one-step method and fermentation media adapted from Shigeo et al (1962) consisting of (in g/l): 60 glucose, 1.2 $(\text{NH}_4)_2\text{SO}_4$, 0.75 KH_2PO_4 , 0.75 K_2HPO_4 , 0.1 $\text{MgSO}_4 \cdot 7\text{H}_2\text{O}$, 0.1 $\text{CaCl}_2 \cdot 2\text{H}_2\text{O}$, 0.005 $\text{FeSO}_4 \cdot 7\text{H}_2\text{O}$ and 0.005 NaCl. A 250 ml unbaffled Erlenmeyer flask was loaded with the medium, sterilized mixed, inoculated with the spore glycerol solution, and stirred (final spore concentration of 240 mg/l or $2.7 \times 10^6 \text{ ml}^{-1}$) and cultivated at $35 \text{ }^\circ\text{C}$ and 150 rpm for ~ 24 hours in an incubator shaker.

There were 2 batches of shake flasks: one set used 240 g/l CaCO_3 , and one set used 192 g/l MgCO_3 for pH buffering, each added at the start of the fermentation to the relevant flask. Both buffers were tested in triplicate. The choice of buffer amounts was 1) to ensure a complete excess of buffer at all times in the system, and 2) to ensure that equivalent amounts of CO_3^{2-} ($\sim 140 \text{ g/l}$) were loaded in both.

2.2 Sample preparation

It was hypothesized that there was a synergistic effect between pH control by $\text{CaCO}_3/\text{MgCO}_3$ dissolution and the precipitation of calcium salts (calcium-malate, -citrate, -fumarate). Due to this, the concentration of acids in the fermentation broth would be lower which in turn would allow *A. oryzae* to continue producing acid without possible adverse effects (pH, osmotic pressure, etc.). To determine how much acid, if any, had precipitated out of solution in the form of calcium/magnesium salts, 2 sets of HPLC and ICP-OES analyses were run on each sample: before acidification and after acid treatment. For this, a fraction of the supernatant was extracted and used for metabolite and cation analyses before acidification. Each sample remnant was then treated with 1 M HCl and incubated in the oven at $90 \text{ }^\circ\text{C}$ for 30 min (vortexed every 5 min) and then centrifuged. The subsequent supernatant was used for metabolite and ICP-OES analyses.

2.3 Analytical methods

Samples from the flasks were collected in pre-weighed CELLSTAR® tubes (Greiner Bio-One, Sigma Aldrich, St. Louis, MO, USA). The concentrations of glucose, glycerol, ethanol, and organic acids in the samples were determined with an Agilent 1260 Infinity HPLC (Agilent Technologies, Santa Clara, CA, USA) fitted with a refractive index detector. Samples ($\pm 1 \text{ ml}$) were centrifuged at $16\,600 \times g$ for 90 s and filtered with $0.45 \text{ } \mu\text{m}$ Nylon (Ministart®, Sigma Aldrich, St. Louis, MO, USA) syringe filters into HPLC vials and loaded into the autosampler tray of the HPLC. Samples ($5 \text{ } \mu\text{l}$) were injected into a Micro-Guard® Cartridge ($30 \text{ m} \times 4.6 \text{ m}$) that was attached to a $300 \text{ mm} \times 7.8 \text{ mm}$ Aminex HPX-87H ion-exchange column (Bio-Rad Laboratories, Hercules, CA, USA) maintained at $60 \text{ }^\circ\text{C}$. Organic acids and glycerol were measured with mobile phase A ($0.02 \text{ M H}_2\text{SO}_4$) and glucose, lactic acid, and ethanol with mobile phase C ($0.002 \text{ M H}_2\text{SO}_4$) both at a flow rate of 0.6 ml/min . Each sample was analyzed twice: the control supernatant and the pre-treated supernatant. The concentration of calcium and magnesium in the solution was measured using inductively coupled plasma mass spectrometry (ICP-OES, Perkin-Elmer, Waltham, MA, USA) using an Argon plasma to ionize the samples and measure the relevant concentrations. This was repeated for both control and pre-treated samples.

2.4 Curve fitting

Time-dependent concentration profiles were approximated in the GraphPad Prism 7.0 (GraphPad Prism Software, San Diego, CA, USA) environment using a four-parameter logistic function

$$C_i(t) = C_{i,max} + \frac{(C_{i,min} - C_{i,max})}{1 + \left(\frac{t}{t_{50}}\right)^k} \quad (1)$$

Consumption/production rates were determined by differentiating the fitted functions.

3. Results & Discussion

The results for the malic acid concentration curves can be seen in Figure 1(a) for the CaCO₃ experiment and in Figure 1(b) for the MgCO₃ experiment. According to the proposed hypothesis, it was anticipated that the measured malic acid concentration would change significantly between the untreated and acid-treated samples. However, a Wilcoxon matched-pairs signed-rank test ($\alpha = 0.05$) showed that there was not a statistically significant difference for the CaCO₃ ($Z = 0.257$; $p = 0.7969$) or MgCO₃ ($Z = 0.873$; $p = 0.383$) sets. This suggested that calcium-malate and magnesium-malate were not present in as significant concentrations as previously predicted. This contradicted the hypothesis that the precipitation of insoluble acid salts decreased the acid concentration in the fermentation broth which would decrease the inhibition of further acid production and therefore the effect of the CaCO₃ or MgCO₃ was likely related to either the supply of CO₂ for anaplerotic reactions required for malate synthesis (Kövilein et al., 2021) or the effect of the alkaline earth cation identity itself.

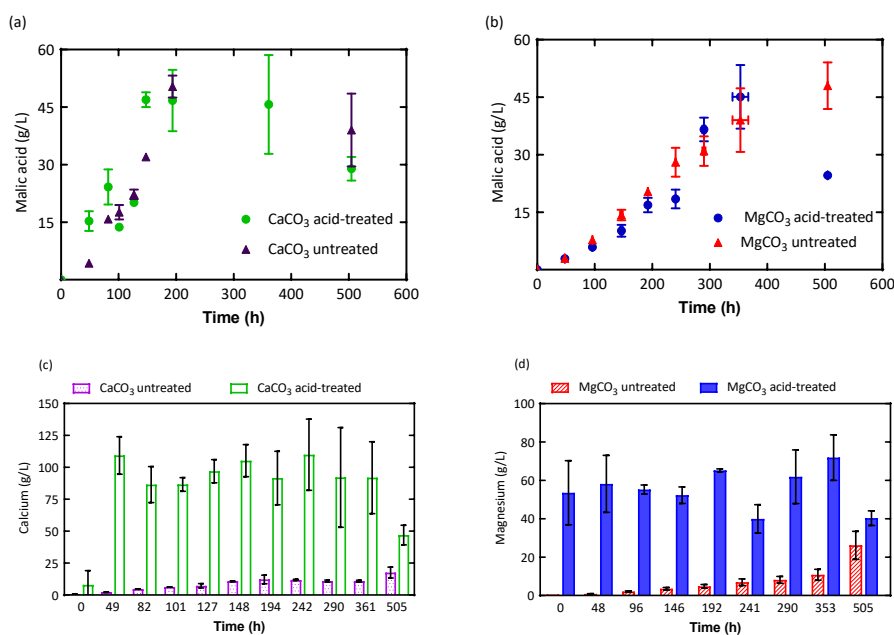


Figure 1: Malic acid concentration curves for (a) CaCO₃ and (b) MgCO₃ shake flask experiments showing untreated and acid-treated measurements. The ICP-MS measured concentrations of each buffer cation in the solution for (c) CaCO₃ and (d) MgCO₃, including the untreated (aqueous cation) and acid-treated (total cation) measurements. Error bars indicated the standard deviation of triplicates.

The calcium and magnesium concentrations measured with ICP-OES can be seen in Figures(c) and (d) below for the untreated and acid-treated samples. As more of the buffer dissolved to neutralize the pH, the concentration of the relevant cation in the solution increased, corresponding to a continuously increasing amount of buffer dissolution as a result of either the neutralization of the acids produced and/or the replacement of CO₂ (in the form of HCO₃⁻) consumed during the biosynthesis of malate (and minor amounts of succinate) during fermentation. The pH for both fermentations had average values of 6.9±0.5 and 8.0±0.5 for the CaCO₃ and MgCO₃, respectively, indicating that the predominant carbonic for was HCO₃⁻. Therefore, the neutralization of

the produced organic acids required one carbonate ion for every proton neutralized. In addition, all produced acids would be fully dissociated for the pH range. From the results, it was observed that 0.88 ± 0.22 M and 1.08 ± 0.30 M of CO_3^{2-} were liberated in the CaCO_3 and MgCO_3 runs, respectively. In comparison, total proton production of 0.79 ± 15 M and 0.80 ± 0.05 M were measured for the CaCO_3 and MgCO_3 runs, respectively. While CO_2 demands of 0.40 ± 0.08 M and 0.40 ± 0.03 M for the synthesis of malate and succinate were determined. From the known equilibrium reactions for CaCO_3 and MgCO_3 in water (Aina et al., 2020), the neutralization of proton results in an equivalent molar formation of HCO_3^- from CO_3^{2-} resulting in the dissolution of $\text{CaCO}_3/\text{MgCO}_3$. In addition, the assimilation of CO_2 (as HCO_3^-) by the fungi results in an equivalent decrease in HCO_3^- in solution which results in the conversion of CO_3^{2-} to HCO_3^- with the concomitant dissolution of $\text{CaCO}_3/\text{MgCO}_3$ to satisfy the prevailing equilibrium conditions.

Therefore, it can be seen that nearly all the CO_2 for anaplerotic reactions was obtained from MgCO_3 , while a very small fraction of CO_2 for these reactions came from CaCO_3 . This implies that the main source of CO_2 for malate synthesis in the CaCO_3 was respiration, while in the MgCO_3 system this was satisfied by the buffer.

The results further demonstrate that a nearly constant concentration of calcium (as Ca^{2+} and CaCO_3) and magnesium (as Mg^{2+} and MgCO_3) were continuously present in the system, corresponding to an average of 96.2 ± 20.1 g/l and 55.4 ± 13.2 g/l for Ca^{2+} and Mg^{2+} , respectively. These values correspond well with the originally loaded amounts of these ions.

The fitted malic acid concentration curves with their corresponding malic acid production rates can be seen in Figures(a) and Figure 2(b). The glucose concentrations for control samples can be seen in Figure 2(c) with the consumption rate curves in Figure 2(d). The fitted parameters were summarised in Table 1. The CaCO_3 set had significantly higher rates of glucose consumption and malic acid production compared to the MgCO_3 set. Despite this, the measured malic acid concentrations were similar between the MgCO_3 and CaCO_3 experiments and the distributions in the group did not differ significantly (Mann-Whitney $U = 32.5$; $n_1 = 9$; $n_2 = 8$; $p = 0.765$ two-tailed). This indicated that the identity of the corresponding metal cation (Ca^{2+} or Mg^{2+}) influenced the production/consumption rates. The glucose was completely consumed for the CaCO_3 set after 250 hours with a decrease in malic acid seen after the same time.

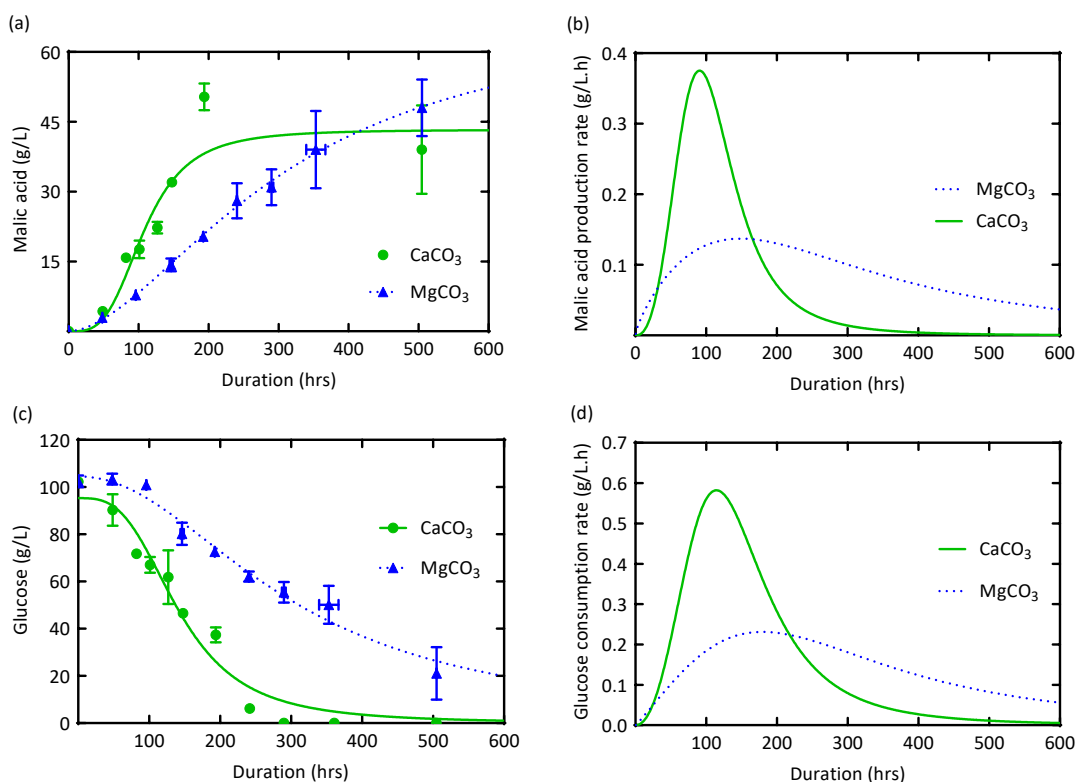


Figure 2: Malic acid (c) concentration curves and (d) production rate curves, glucose (e) concentration curves, and (f) consumption rate curves for the MgCO_3 and CaCO_3 control shake flask experiments. Curves were fitted using the logistic model (Equation 1) with the standard deviation of triplicates shown by the error bars.

Table 1: Curve fitting parameters for the concentration profiles in Figures (a) and (c)

Dataset	240 g/l CaCO ₃		192 g/l MgCO ₃	
	Glucose	Malic acid	Glucose	Malic acid
$C_{i,min}$ (g/l)	0	0	0	0
$C_{i,max}$ (g/l)	95.3	43.3	105	68.9
k	-3.12	3.44	-2.07	1.75
rt_{50} (h)	142	108	299	311
R^2	0.956	0.876	0.952	0.958

The results presented in Figures 1 and 2 indicate that the effects of alkaline-earth buffer identity are extremely complicated. The results demonstrated that the hypothesis of immobilization of malate as Ca-malate or Mg-malate was not a significant factor in the system as negligible amounts of these complexes were detected. However, from the ionic dissolution measurements, it appeared that the type of buffer affected the source of the CO₂ required for malate biosynthesis. This links strongly to the significantly increased rate of glucose consumption, with concomitant increased respiration rate, when comparing the CaCO₃ and MgCO₃ runs.

The Ca²⁺ ion has been labeled the second messenger omnipresent in all fungi (Navazio and Mariani, 2008). This increased Ca²⁺ concentration within the external medium results in a coordinated range of intracellular signals to regulate the Ca²⁺ concentration (Roy et al., 2021), including stimulating the oxidative metabolism within the mitochondria to regulate ATP synthesis (Tarasov et al., 2012). This Ca²⁺ homeostasis and signaling have physiological implications for the growth, virulence, and stress responses in fungi (Lange and Peiter, 2020). These effects contributed to a significantly promoted rate of glucose transfer into the fungal biomass in Ca²⁺ stimulates fungi, while this same observation was not made for Mg²⁺ (Pitt and Ugalde, 1984).

Applying the observed results in Figure 1 and Figure 2 to *A. oryzae*, the symbiotic relationship between CaCO₃ and malic acid could be explained using a calcareous environment as a reference point. *A. oryzae* is part of a genus that is distinct from other microbes: they can utilize both a secondary and primary metabolism (Brown et al., 1996). In the primary metabolism, acidic compounds are secreted for nutrient acquisition from the soil (Wu et al., 2018). Specifically, for the extraction of phosphorous where Ca²⁺ sequesters phosphorus, malate improved the efficiency of phosphorus extraction from the soil (Ström et al., 2005). The secondary metabolism can utilize the acidic compounds from the primary metabolism. This allows *A. oryzae* to produce secondary metabolites that it can utilize to adapt to its current environment and inhibit the primary metabolic pathways (Brown et al., 1996).

MgCO₃ would act similarly when considering a dolomitic soil environment where phosphate would be sequestered by the Mg²⁺ and require a release for phosphorus uptake by the fungi. However, the reduced stimulation of the fungal physiology as compared to the CaCO₃ system resulted in a less pronounced effect of Mg²⁺ on the system. This could be tested in the immobilized bio-reactor using NaOH/Na₂CO₃ to control the pH and spiking with CaCl₂ or MgCl₂.

4. Conclusions

The study presents an investigation of the effect of alkaline earth buffer (CaCO₃ and MgCO₃) on the production of malic acid by *A. oryzae* in a batch bioreaction system. Based on the results, alkaline-earth metals play a key role in the production rate of malic acid with *A. oryzae* NRRL 3488. The glucose consumption and utilization were higher when CaCO₃ was used as a buffer compared to MgCO₃, however, similar amounts of malic acid were produced. This study provides invaluable insights into this potentially lucrative yet relatively simple avenue for the improvement of malic acid production by *A. oryzae*. However, it is clear that the production of malic acid by *A. oryzae* is a complex, multi-faceted problem requiring understanding of the physiological interactions of the biocatalyst with its environment. The current study is limited to a batch reaction system at laboratory scale and therefore larger scale study is an imperative before real-world application can be realised.

Nomenclature

$C_i(t)$ – time-dependent concentration of component i , g/l

$C_{i, min}$ – minimum concentration of component i , g/l

$C_{i, max}$ – maximum concentration of component i , g/l

k – parameter describing the shape of the model curve

t_{50} – processing time required to reach the mid-point of the concentration curve, h

References

- Aina S.T., Du Plessis J.B., Mjimba V., Brink H.G., 2020, Effect of Membrane Removal on the Production of Calcium Oxide from Eggshells via Calcination. *Chem. Eng. Trans*, 81, 1069–1074.
- Brown D.W., Adams T.H., Keller N.P., 1996, *Aspergillus* has distinct fatty acid synthases for primary and secondary metabolism. *Proc. Natl. Acad. Sci.*, 93, 14873–14877.
- Chi Z., Wang Z.P., Wang G.Y., Khan I., Chi Z.M., 2016, Microbial biosynthesis and secretion of L-malic acid and its applications. *Crit. Rev. Biotechnol.*, 36, 99–107.
- Geyer M., Onyancha F.M., Nicol W., Brink H.G., 2018, Malic acid production by *aspergillus oryzae*: The role of CaCO₃. *Chem. Eng. Trans.*, 70, 1801–1806.
- Hermann B.G., Patel M., 2007, Today's and tomorrow's bio-based bulk chemicals from white biotechnology. *Appl. Biochem. Biotechnol.*, 136, 361–388.
- Knuf C., Nookaew I., Remmers I., Khoomrung S., Brown S., Berry A., Nielsen J., 2014, Physiological characterization of the high malic acid-producing *Aspergillus oryzae* strain 2103a-68. *Appl. Microbiol. Biotechnol.*, 98, 3517–3527.
- Kövilein A., Umpfenbach J., Ochsenreither K., 2021, Acetate as substrate for L-malic acid production with *Aspergillus oryzae* DSM 1863. *Biotechnol. Biofuels*, 14, 1–15.
- Lange M., Peiter E., 2020, Calcium Transport Proteins in Fungi: The Phylogenetic Diversity of Their Relevance for Growth, Virulence, and Stress Resistance. *Front. Microbiol.*, 10.
- Liu J., Xie Z., Shin H. dong, Li J., Du G., Chen J., Liu L., 2017, Rewiring the reductive tricarboxylic acid pathway and L-malate transport pathway of *Aspergillus oryzae* for overproduction of L-malate. *J. Biotechnol.*, 253, 1–9.
- Liu J., Li J., Shin H. dong, Du G., Chen J., Liu L., 2018, Biological production of L-malate: recent advances and future prospects. *World J. Microbiol. Biotechnol.*, 34, 1–8.
- Melo A.F., Mauricio E.F., Salgado A.M., Pellegrini Pessoa F.L., Triches Damaso M.C., Couri S., 2011, Assessment of catalytic properties in aqueous and media of *aspergillus niger* lipase immobilized on supports vitreous. *Chem. Eng. Trans.*, 24, 973–978.
- Mondala A.H., 2015, Direct fungal fermentation of lignocellulosic biomass into itaconic, fumaric, and malic acids: current and future prospects. *J. Ind. Microbiol. Biotechnol.*, 42, 487–506.
- Navazio L., Mariani P., 2008, Calcium opens the dialogue between plants and arbuscular mycorrhizal fungi. *Plant Signal. Behav.*, 3, 229–230.
- Ochsenreither K., Fischer C., Neumann A., Sylđatk C., 2014, Process characterization and influence of alternative carbon sources and carbon-to-nitrogen ratio on organic acid production by *Aspergillus oryzae* DSM1863. *Appl. Microbiol. Biotechnol.*, 98, 5449–5460.
- Park Y., Kang S., Lee J., Hong S., Kim S., 2002, Xylanase production in solid state fermentation by *Aspergillus niger* mutant using statistical experimental designs. *Appl. Microbiol. Biotechnol.*, 58, 761–766.
- Payne G.A., Nierman W.C., Wortman J.R., Pritchard B.L., Brown D., Dean R.A., Bhatnagar D., Cleveland T.E., Machida M., Yu J., 2006, Whole genome comparison of *Aspergillus flavus* and *A. oryzae*. *Med. Mycol.*, 44, 9–11.
- Pitt D., Ugalde U.O., 1984, Calcium in fungi. *Plant, Cell Environ.*, 7, 467–475.
- Roy A., Kumar A., Baruah D., Tamuli R., 2021, Calcium signaling is involved in diverse cellular processes in fungi. *Mycology*, 12, 1–15.
- Shigeo A., Furuya A., Saito T., 1962, Method of producing L-malic acid by fermentation. United States.
- Smith C.S., Slade S.J., Nordheim E. V., Cascino J.J., Harris R.F., Andrews J.H., 1988, Sources of Variability in the Measurement of Fungal Spore Yields. *Appl. Environ. Microbiol.*, 54, 1430–1435.
- Ström L., Owen A.G., Godbold D.L., Jones D.L., 2005, Organic acid behaviour in a calcareous soil implications for rhizosphere nutrient cycling. *Soil Biol. Biochem.*, 37, 2046–2054.
- Tarasov A.I., Griffiths E.J., Rutter G.A., 2012, Regulation of ATP production by mitochondrial Ca²⁺. *Cell Calcium*, 52, 28–35.
- Werpy T., Petersen G.R., 2004, Top value added chemicals from biomass. Volume 1-results of screening for potential candidates from sugars and synthesis gas. National Renewable Energy Laboratory, Golden.
- Wu L., Kobayashi Y., Wasaki J., Koyama H., 2018, Organic acid excretion from roots: a plant mechanism for enhancing phosphorus acquisition, enhancing aluminum tolerance, and recruiting beneficial rhizobacteria. *Soil Sci. Plant Nutr.*, 64, 697–704.